

Design and Fabrication of Abrasive Jet Machine

**A THESIS SUBMITTED IN PARTIAL FULFILLMENT OF
THE REQUIREMENT FOR THE AWARD OF THE DEGREE
OF
MASTER OF TECHNOLOGY
IN
MECHANICAL ENGINEERING
(SPECIALIZATION IN PRODUCTION ENGINEERING)
BY
JUKTI PRASAD PADHY
(ROLL NO. 211ME2353)**



**DEPARTMENT OF MECHANICAL ENGINEERING
NATIONAL INSTITUTE OF TECHNOLOGY
ROURKELA-769008, ODISHA
INDIA (2013)**

Design and Fabrication of Abrasive Jet Machine

**A THESIS SUBMITTED IN PARTIAL FULFILLMENT OF
THE REQUIREMENT FOR THE AWARD OF THE DEGREE
OF
MASTER OF TECHNOLOGY
IN
MECHANICAL ENGINEERING
(SPECIALIZATION IN PRODUCTION ENGINEERING)
BY
JUKTI PRASAD PADHY**

(ROLL NO. 211ME2353)

Under the Guidance of

Dr. C.K. Biswas

Department of Mechanical Engineering



**DEPARTMENT OF MECHANICAL ENGINEERING
NATIONAL INSTITUTE OF TECHNOLOGY
ROURKELA-769008, ODISHA
INDIA (2013)**



Department of Mechanical Engineering
National Institute of Technology
Rourkela

CERTIFICATE

This to certify that the thesis entitled “*Design and Fabrication of Abrasive Jet Machine*” being submitted by **Mr Jukti Prasad Padhy** in partial fulfillment of the requirements for the award of Master of Technology in Mechanical Engineering with “Production Engineering” Specialization during session 2009-2010 in the Department of Mechanical Engineering National Institute of Technology, Rourkela.

It is an authentic work carried out by him under my supervision and guidance. To the best of my knowledge, the matter embodied in this thesis has not been submitted to any other University/Institute for award of any Degree or Diploma.

Date

Dr. C. K. Biswas

Associate Professor

Department of Mechanical Engineering

National institute of technology, Rourkela

ACKNOWLEDGEMENT

I express my deep sense of gratitude and indebtedness to my thesis supervisor Dr. C. K. Biswas, Associate Professor, Department of Mechanical Engineering for providing precious guidance, inspiring discussions and constant supervision throughout the course of this work. His timely help, constructive criticism, and conscientious efforts made it possible to present the work contained in this thesis.

I express my sincere thanks to Mr. Shailesh Kumar Dewangan and Mr. Shatabdi Biswal. My sincere gratitude thanks to Mr. Kunal. Nayak, and Mr. Arabinda Khuntia Technical Assistance in Production Engineering lab. I am grateful to Prof. K.P. Maity, Head of the Department of Mechanical Engineering for providing me the necessary facilities in the department. I express my sincere gratitude thanks all my Family member well-wishers for their inspiration and help.

I feel pleased and privileged to fulfill my parent's ambition and I am greatly indebted to them for bearing the inconvenience during my M Tech. course.

Date

Jukti Prasad Padhy

211me2353

Abstract

Abrasive Jet Machining (AJM) is a non-conventional machining process where a high-pressure air stream with small abrasive particles to impinge the work surface through a nozzle. A CNC milling machine was modified to an AJM, using the C-frame, X-Y table, stepper motor and other parts of the CNC.

Using CAD software, CATIA and AUTOCAD, a model of AJM was designed. The working chamber and nozzle holding arrangement was fabricated in our institute work shop. Cheap and easily available material like aluminum sheet, steel rod, mild steel, glass fiber, polythene sheet, alien bolt and spring are used for fabrication of machining component. The controller, nozzle, abrasive powder, hose pipe, FRL unit was bought from market.

The machine automation was done by using the controller and driver circuit. By feeding the different programing, complicated model was machined.

After completing the fabrication work, drilling experiment was done on glass as the work piece and aluminum oxide (Al_2O_3) as abrasive powder. The effect of Overcut (OC) and Material removal rate (MRR) of glass material was finding by using L_9 orthogonal array based on Taguchi design and considering the, pressure of air and stand-off-distance are control parameter.

Keyword- Abrasive jet machining, FRL Unit, enclosure, Mixing chamber, Taguchi method

Table of Contents

CERTIFICATE	I
ACKNOWLEDGEMENT	II
Abstract	III

Chapter 1 Introduction

1.1. History of AJM	1
1.2. Principle of AJM	2
1.3. Process description	2
1.4. Material removal rate	5
1.5. Application	6
1.6. Advantages	7
1.7. Disadvantages	7

Chapter 2 Literature review

2.1. Literature review	8
2.2. Motivation of present work	12

Chapter 3 Design and fabrication

3.1. Methodology	13
3.2. Working chamber	13
3.2.1 Enclosure	15
3.2.2 Work holding devices	16
3.2.3 Opening and closing system	16
3.2.4 Drainage system	17
3.3. Air compressor	17
3.4. FRL unit	18
3.5. Mixing chamber	19
3.6. Nozzle and its holding arrangement	19

3.7.	Piping circuit.....	20
3.8.	Machine automation.....	21
3.9.	Controller	21
3.10.	Stepper motor.....	22
3.11.	Machine Frame and X-Y-Z Travel	22
3.12.	Assembly.....	23
3.13.	Conclusion	24

Chapter 4 Experimentation

4.1.	Introduction.....	25
4.2.	Selection of the work piece and abrasive powder	25
4.3.	Material removal rate	26
4.4.	Overcut.....	26
4.5.	Flow Chart of Experiment.....	27
4.6.	Design of experiments (DOE).....	28
4.7.	Taguchi design	28
4.8.	Conduct of experiment.....	29
4.9.	Design of observation table.....	32
4.10.	Conclusion	32

Chapter 5 Result and dissections

5.1.	Introduction.....	33
5.2.	Influences of MRR.....	33
5.3.	Influences of OC	38
5.4.	Conclusion	43

Chapter 6 Conclusion

6.1.	Conclusion based on fabrication work.....	44
6.2.	Scope for future work	45
	References.....	46

List of Figure

Fig.1.1 Schematic diagram of AJM	2
Fig.1.2 Line diagram of AJM	3
Fig.1.3 Effect of process parameter on MRR	6
Fig. 3.1 Modeled view of working chamber.....	14
Fig. 3.2 Full view of working chamber.....	14
Fig. 3.3 Full view of air compressor	18
Fig. 3.4 Full view of FRL unit	18
Fig.3.5 Full view of mixing chamber	19
Fig.3.6 Modeled view of mixing cylinder	19
Fig.3.7 Modeled view of nozzle and its holder	20
Fig.3.8 Full view of nozzle and its holder	20
Fig 3.9 Nylon braided hose pipe	20
Fig 3.10 Full view of controller	21
Fig 3.11 Circuit connection.....	21
Fig 3.12 Modeled view of AJM.....	23
Fig. 3.13 Front view of AJM	23
Fig. 3.14 Side view of AJM.....	23
Fig 4. 1 Experimental set up	30
Fig. 4.2 Electronic balance or weight machine.....	30
Fig. 4.3 Optical microscope	30
Fig. 4.4 Tool maker microscope	30

Fig. 4.5 Drilled cavity on work piece (run numbers are indicated)	31
Fig. 4. 6 View of nozzle dia before experiment	31
Fig. 4. 7 View of nozzle dia. after experiment.....	31
Fig 5. 1 Main effect plot for mean of MRR.....	34
Fig 5. 2 The residual plot for mean of MRR.....	37
Fig 5. 3 Contour plot of MRR.....	37
Fig 5. 4 Surface plot of MRR.....	37
Fig. 5.5 Main effect plot of mean for OC	39
Fig. 5. 6 Residual plot for OC.....	42
Fig. 5. 7 Contour plot for OC.....	43
Fig 5. 8 Surface plot for OC.....	43

List of Table

Table 1.1 Process parameter and its standard value	4
Table 3.1 Material required for made of working chamber	15
Table 4.1 Properties of glass	25
Table 4.2 Properties of abrasive powder.....	25
Table 4.3 Machining parameters and their level.....	29
Table 4.4 Design of observation table	32
Table 5.1 Observed value of MRR	33
Table 5.2 Analysis of variance for MRR	35
Table 5.3 Response table for MRR.....	36
Table 5.4 Estimated Model Coefficients for MRR.....	36
Table 5.5 Observed value of OC.....	39
Table 5.6 Analysis of variance for OC	40
Table 5.7 Response table for OC	40
Table 5.8 Estimated Model Coefficients for OC	41

1.1. History of AJM

The sand blasting machine used, developed by Benjamin Tilghman in 1870, for removal of painted and rusted surface of a material before making another practical use. Thomas Pangborn expanded the sand blast technique using of compressed air in combination with the sand in 1904, after that Sandblasting are typically composed of an air compressor, abrasive particle and a blaster nozzle. Basically this is used for cleaning the surface of any materials before decoration or usage, or etching the textured designs of a given material for good appearance. Originally, the process had occurred the use of sand, but later this method was changed because of the inhalation of sand particles creates seriously respiratory problem on the lungs and makes disease called silicosis.

In 1893, the air processor rendered the sandblasting technique employable for industrial usage on a wider scale. In 1918, the enclosure was built for shielding the sand blasting process. In 1939, various small and uniform particles such as aluminum oxide, silicon carbide, quartz, glass particle, steel grit, and even walnut shells, coconut shells have been used in sandblasting technique based upon their requirement. Though different abrasive particle used in this technique called as abrasive blasting.

At first abrasive blasting was used in the industry purposes such as removing rust or finishing of metal before using in the practical purpose .in the later stage the technique also used in the decorating of the material.

For machining the various ceramic and brittle materials, in later stage very small size abrasive particle, small nozzle, high compressed air is used. And this technique is called micro abrasive blasting or abrasive jet machining.

1.2. Principle of AJM

AJM is also named as abrasive micro blasting, is a nonconventional machining process that carried a high-pressure air stream with small abrasive particles to impinge the work surface through a nozzle for material removal of the work piece.

The material removal occurs by the erosive action of the abrasive particles striking the work piece surface. The material removal capability of AJM is very low so it is used in a finishing process. It is as an effective machining method for hard and brittle materials . and it's it is similar to sand blasting process but difference is finer abrasive powders and smaller nozzles are used in AJM.

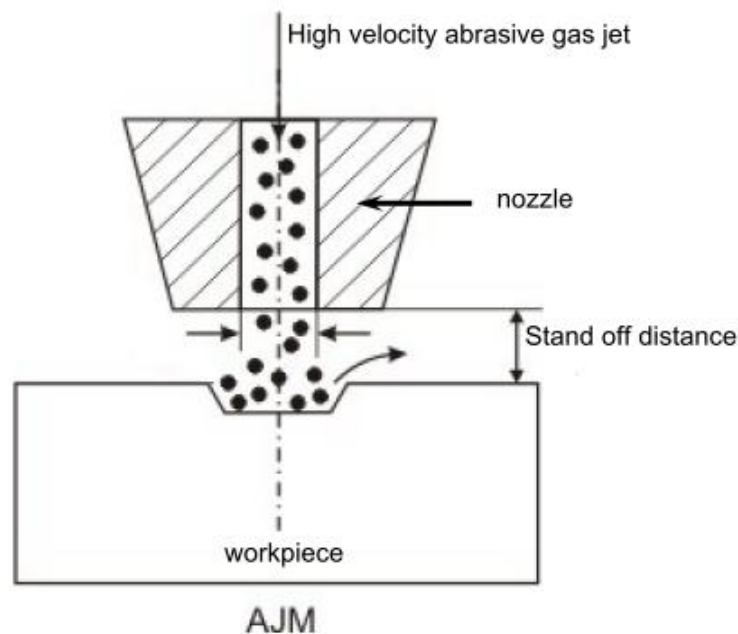


Fig.1. 1 Schematic diagram of AJM

1.3. Process description

A schematic diagram of AJM is shown in Fig. 1.1 in AJM; carrier gas is compressed at a high pressure in an air compressor. Gases like dry air, CO₂, N₂ are used as a carrier gas. At first

the carrier gas is passed through a pressure regulator to obtain the desired working pressure. The gas is then passed through a FRL unit (filter lubricator and regulator). This unit removes dust particle and also lubricate and regulate the flow of carrier gas. After that the carrier gas enters into the mixing chamber. The abrasive particles placed in the abrasive container. Abrasive particle are enter into the mixing chamber as per our requirement by the application of vibrator. The abrasive particles are then carried by the carrier gas from the mixing chamber to work piece through nozzle. The total machining process is enclosed for safe and ecofriendly purpose. line diagram of AJM is indicated in the Fig.1. 2.

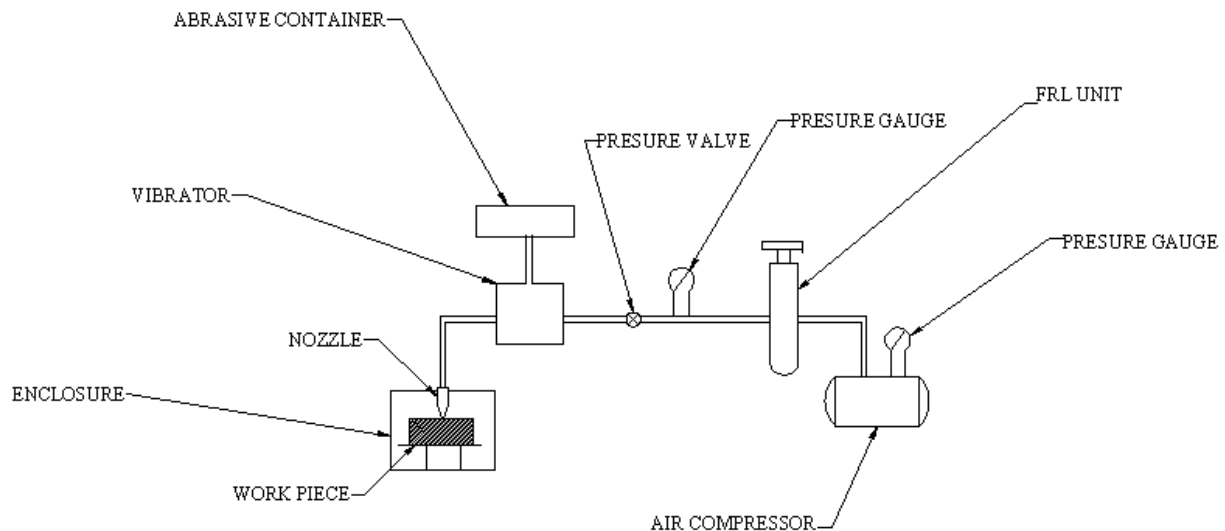


Fig.1. 2 Line diagram of AJM

The major components are:

- Compressor.
- FRL unit
- Pressure Gauge.
- Pressure Valve.
- Abrasive Container.
- Vibrator or Mixer.
- Nozzle.

- Enclosure
- Work Piece
- Abrasive Powder

The process parameter and its standard value are in given in Table 1.1 that is required for experimental work.

Table 1. 1 Process parameter and its standard value

Abrasive powder	Shape	Irregular or spherical
	Size	10-50 μ m
	Flow rate	5- 20 gm/min
	Material	AL ₂ O ₃ , SiC
Carrier gas	Composition	Air, CO ₂ , N ₂
	Velocity	500-700 m/s
	Pressure	2-10 bar
	Flow rate	5-30 lpm
Abrasive et	Velocity	100-300 m/s
	Mixing ratio	M _{abr} /M _{gas}
	Stand-off distance	0.5-5 mm
	Impingement angle	60 ⁰ -90 ⁰
Nozzle	Material	Tungsten carbide, boron carbide, sapphire
	Diameter	0.2-0.8 mm
	Life	10-300 hr

Machining Parameter

- Work piece
 - Material removal rate

- Surface roughness
- Nozzle
 - Wear rate

1.4. Material removal rate

The material removal takes place from the work piece by the application high velocity abrasive jet particle. Due to the kinetic energy of particle causes erosion of work piece .The material removal is depend upon the certain parameter such as abrasive flow rate, mixing ratio, gas pressure, stand-off distance etc. The MRR depends on different process parameter. The Fig.1. 3 shows that

- Material removal rate (MRR) increases with increase of abrasive flow rate due to the more number of particle impingement in unit time But after reaching a optimum value material removal rate decreases with further increase of abrasive flow rate because of mass flow rate of gas decreases with increase of abrasive flow rate.
- Similarly Material removal rate (MRR) increases with increase of mixing ratio (M_{abr}/M_{gas}). But after reaching a optimum value material removal rate decreases with further increase of mixing ratio.
- Material removal rate (MRR) continuously increases with increase in abrasive flow rate when mixing ratio is kept constant.
- Material removal rate (MRR) increases with increase of gas pressure.
- At first Material removal (MRR) rate increases with increase in stand-off distance then it is remains constant for a period of time and after that decreases with increase in stand -off distance. This phenomena occurs due to penetration rate of abrasive material is optimum at certain level. After that it will decreases.

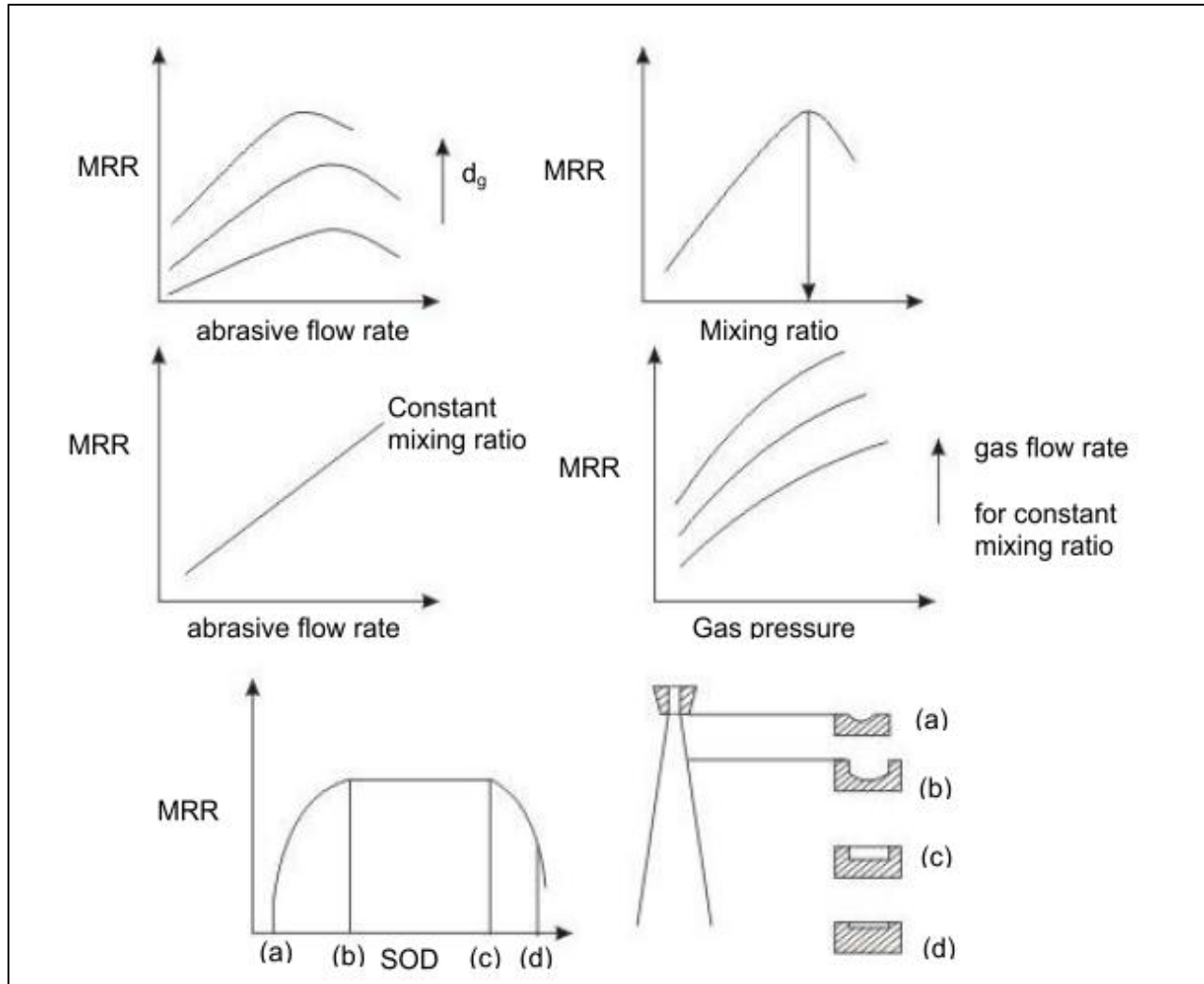


Fig.1. 3 Effect of process parameter on MRR

1.5. Application

- It is mainly used to machining of brittle, fragile and heat sensitive material such as glass, ceramic, sapphire and quartz.
- Used for removing of oxide on metal and resistive coating of metal.
- Suitable for cutting of thin fragile component such as silicon and germanium
- Also used for manufacturing of nylon and Teflon component ,making of electronics device

- it is also useful for drilling , polishing , cutting , etching deburring of hard and brittle materials

1.6. Advantages

- Capital cost is low
- Easier to operate and maintain.
- It is free from chatter and vibration.
- Absence of contact between the tool and work piece so there is no chance of tool damage.
- By changing the grain size better surface finish is obtained.

1.7. Disadvantages

- Application is limited due to low material removal rate.
- Chances of embedding of abrasive particle into the work piece when soft material is machining
- Risk of environment pollution and health hazard is higher
- Reusing of abrasive particle is difficult
- The air is fully demisting otherwise there is a chance of accumulation of abrasive particle at the nozzle.

2.1. Literature review

The literature survey of Abrasive Jet Machine says that the Abrasive Jet Machining process was started a few decades ago. Till today experimental and theoretical study on the Abrasive Jet Machining process occurs. Most of the study based upon experiment. Some of the study based upon modeling and analysis.

Ke et.al [1] has designed a novel hybrid method, called flexible magnetic abrasive jet machining, for investigating the machining characteristics of the self-made magnetic abrasive in abrasive jet machining. According to Taguchi method conclusion was derived that flexible magnetic abrasive particle gives better MRR and surface roughness than traditional abrasive.

Wang and fan [2] represented a theoretical analysis and associated with mathematical models for the velocity of abrasive particles in an abrasive air jet machining. By using the Bernoulli's equation of compressible of flow jet air velocity was calculated. Considering particle mean diameter, nozzle length, air density and air flow velocity particle velocity at the nozzle exit is determined. Also modeled the distribution of particle velocities along the jet centerline downstream from the nozzle and the particle velocity profile at a jet cross-section by considering surrounding air entrainment and air-particle interaction. After comparing the experimental result with theoretical calculation, it was shown that less than 4% error was occurred.

Gradeena et.al [3] used a cryogenic abrasive jet machining apparatus for solid particle erosion of polydimethylsiloxane (PDMS) using aluminum oxide as an abrasive at a temperature range between -178°C to 17°C . He observed that optimum machining of PDMS occurred at temperature approximately at -178°C and the attacking angle in between 30° to 60° . They were also found that PDMS can be machined above its glass transition temperature.

Ally et.al [4] observed that the optimum erosion rate occurred at impact angles between of 20° – 30° when machining the aluminum 6061-T6, 316L stainless steel and Ti–6Al–4V alloy and taking the $50\text{ }\mu\text{m}$ AL_2O_3 abrasive powder. Demonstrating the surface evolution model during the machining process of metal which was originally developed for ductile polymer and found that AJM etch rate in metal was minimum when compared with the glass and polymer.

Tyagi [5] has presented a theoretical study carried out with the help of mathematical model and computational technique of abrasive jet machining which is based on the principal of velocity shear instability, generated by thermionic process. Based upon the plasma factor erosion from metallic surface can be controlled by changing the input parameter such as electric field, magnetic field and shear scale length.

Lin et.al [6] designed a hybrid model based upon combined mechanism of abrasive jet machining (AJM) and electrical discharge machining (EDM). To removing the recast layer of SKD 61 steel during the EDM process in dehumidified gas medium the AJM process was incorporated. The hybrid process not only increases the material removal rate but also generated a fine surface finish.

Dehnadfar et.al [7] has finding out the micro machined surface by applying a jet of particle passed through narrow mask opening in abrasive jet micromachining (AJM). The structure of micro machined feature depends on mass flux and particle velocity. In this experiment shadowgraphy speed laser technique was used to study the size distributions and particle velocity.

Fan et.al [8] has presented a particle image velocimetry (PIV) technique to study the particle velocity in micro abrasive jet machine. He found that particle jet flow has linearly expansion in downstream. Due to the increase in air pressure the particle velocity increases. He considered radial profile and axial in the particle flow field. In the centerline downstream the axial profile has three stages i.e. acceleration stage, a transition stage, and a deceleration stage. For considering the radial velocity profiles, a relatively flat shape is observed near the nozzle exit.

Getu et.al [9] described the cooling of machined surface and also considering optimum cooling that signifies the cost effective. He applied the finite element thermal analysis technique

on CAJM With a view to process optimization, a finite element thermal analysis has been made of the CAJM of holes and channels in polydimethylsiloxane (PDMS).

Burzynski and papini [10] implemented the narrow band level set method (LSM) on AJM for find out the surface evolution on inclined masked micro-channel in poly-methyl-methacrylate (PMMA) and glass. The result profile of glass have round bottom and curved wall and the resulting profile of PMMA have straight walls and rectangular bottoms.

Zhang et.al [11] described about the decreases of machining efficiency in progress of machining when small hole was machined on MAJM, due to the colliding abrasives were accumulated in the bottom of the hole and preventing the direct impact of abrasives onto the work piece. For overcoming this difficulty he used a new technique called Micro Abrasive intermittent jet machining (MAIJM), in this machining a small gap of time given during the machining in which continuous flow of gases occurred without taking of abrasive particle.

Ghobeity et.al [12] presented a analytical models on AJMM in which the target is oscillated transversely to the overall scan direction, by which they predicted the shape, sidewall slope, and depth of machined planar areas and transitional slopes in glass.

Wakuda et.al [13] compared the machinability between AJM process and the solid particle erosion model. They concluded from the test result that the relative hardness of the abrasive against the target material is critical in the micro-machining process but it is not taken into consideration. In conventional erosion process radial crack do not propagate downwards as a result of particle impact due to no strength degradation occurs for the AJM surface.

Park et.al [14] described that the performance of MAJM in the micro-grooving of glass. They takes the diameter of the hole-type and the width of the line-type groove are 80 μm . according to the experimental result they concluded that the size of machined groove increased about 2–4 μm . they suggest that using of masking process and the compensation for film wear, MAJM process was effectively used in the machining of electronic device, LCD and semiconductor.

Shafiei et.al [15] developed computer simulation model to predict the time evolution of the eroded profiles on machined surfaces, which is a function of machining parameters such as,

inclination and distance to target surface, abrasive nozzle size, size, abrasive jet particle velocity and flux distribution. They also calculated the effect of collisions between incoming and rebounding particles by tracking the individual particles, performing inter-particle and particle to surface collision detection.

Barletta and Tagliaferri [16] define a relatively novel machining technology known as fluidized bed assisted abrasive jet machining (FB-AJM) for finishing the internal part of long and narrow tubular parts made by stainless steel. They found out the surface roughness and material removal rate by analyzing the machining mechanism and Experimental investigating.

Li et.al [17] determined the particle velocities at the nozzle exit based on the nozzle length particle mean diameter, air density, particle density and air flow velocity. Also modeled a numerical solution for determine the particle velocities by dividing the nozzle and the jet flow in air into small segments along the jet axial direction and it is verified with the calculated particle velocities from a particle image velocimetry (PIV) measurement of the velocity distribution in micro-abrasive air jets.

Jianxinn et.al [18] developed a (W, Ti) C/SiC ceramic composite nozzle, investigated the erosion wear behavior and compared with conventional ceramic nozzle. They concluded that composite nozzle exhibit high erosion wear resistance than the conventional.

Jafar et.al [19] developed a numerical model to simulate the brittle erosion process leading to the creation of unmasked channels as a function of velocity, particle size, dose, and impact angle and target material properties. The result indicates that chip removal of borosilicate glass was achieved by lateral cracking. The edge chipping normally occurred when the impact angle was so small and helpful for making smooth profile.

Achtsnick et.al [20] had set a model containing different sub model containing the particle jet, the machining result and erosion mechanism of a single particle impact. The simulation shows the Laval-type nozzle. A one-dimensional isentropic flow model was developed to calculate the particle exit velocity of each individual particle in the air flow for two different types of nozzles: a converging cylindrical and a new developed line shaped Laval-type nozzle have more than 30% particle velocity compared to the converging nozzle. They also verify the

experimental result by using particle image velocimetry (PIV). By Roughness measurement and the blasting profile shape, conclusion was derived that this model gave result accurately.

Jianxin [21] studied the erosion wear behavior of boron carbide nozzles, using the silica, siliconcarbide and alumina powder as abrasive, on abrasive jet machining. Conclusion was derived that the hardness of abrasive particle was played an important role on wear behavior boron carbide nozzle. Boron carbide nozzle was produced by hot pressing.

2.2. Motivation of present work

Not only developing of innovative shape design of product and its component but also new exotic alloy material creates lots of pressure on conventional machining. At the same time electro chemical machining and electro discharge machining are limited using on conductive material and makes high initial and operation cost also. Similarly chemical etching requires high technical knowledge, strictly obeying the safety guidelines. plasma arc machining, electron beam machining laser beam machining etc. requires high investment and operating cost , requiring of high skilled operator and also various limitation motivates use of abrasive jet machining.

AJM was not available in our production laboratory. So there was much difficulty to machining of glass, ceramic and brittle material. The AJM cost is very high in the market. To overcome such difficulty, motivate towards fabrication of new AJM machine. And the fabrication cost is much lower than the cost of new AJM machine.

3.1. Methodology

A CNC milling machine was modified to an AJM, using the C-frame, X-Y table, stepper motor and other parts of the CNC. The fabrication was done in our production lab by using conventional machine tool which is available in our institute workshop.

Firstly, identifying the component which was necessary for fabrication. Then design the entire component by using cad package software like AutoCAD and catia. Most of the component was designed by using catia software. Then make categorizing the component based upon manufacturing in workshop, available in production lab and market. Care was taken so optimum using of space and material which are available in our production lab. The material used for manufacturing of component are mild steel, aluminum sheet, glass fiber , alien bolt, rubber, spring etc. List of the components are used for fabrication of AJM

- Working chamber
- Mixing chamber
- FRL unit
- Nozzle and its holding arrangement
- Compressor
- Control unit
- Hose pipe circuit
- Table movement

3.2. Working chamber

It is the main part of fabrication system which is made in the production laboratory. Before goes to fabrication, different component were designed in the catia software, which is shown in the figure 3.1. Based upon the modeled it was fabricated in our workshop which is shown in the figure 3.2.

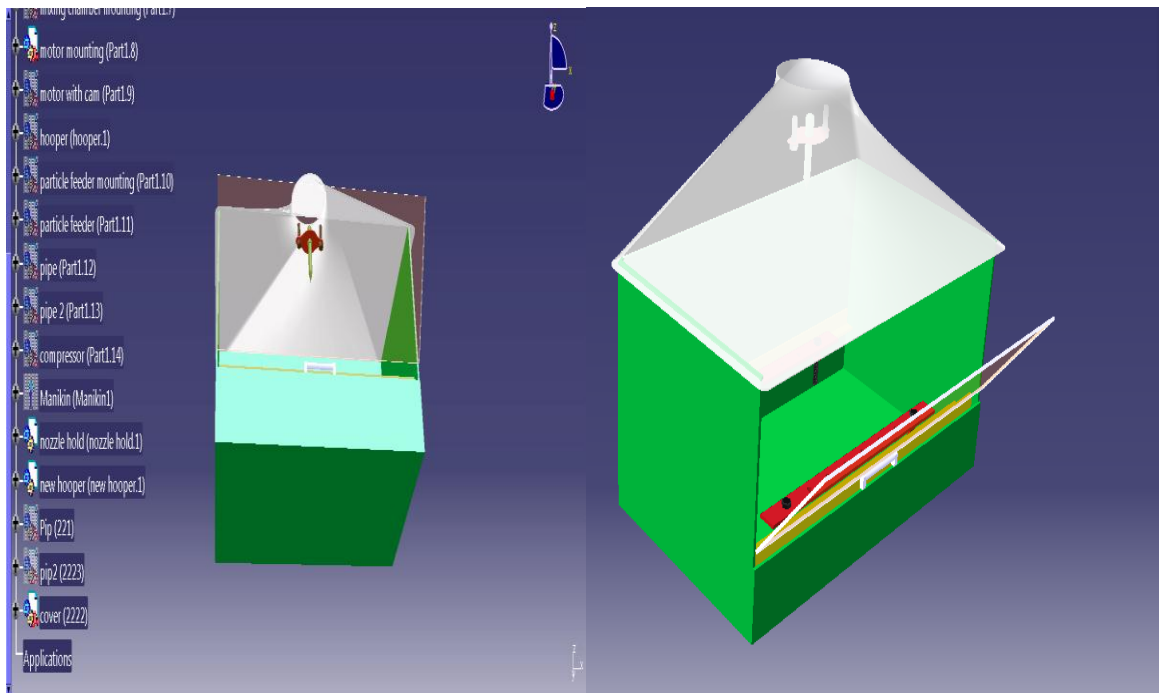


Fig. 3.1 Modeled view of working chamber

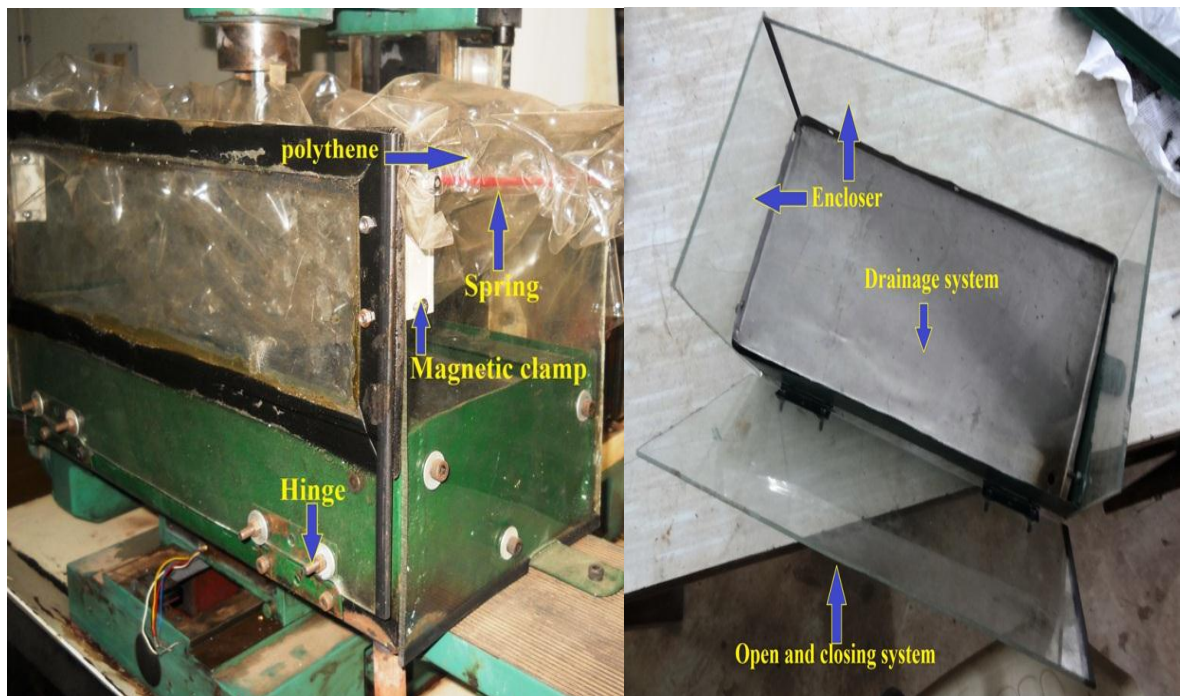


Fig. 3.2 full view of working chamber

Different component of working chamber

- Enclosure
- Work holding devices
- Opening and closing system
- drainage system

For fabrication of enclosure different raw material is used, the list of the different material is given in the table 3.1.

Table 3. 1 Material required for made of working chamber

Sl. No	Raw material	Specification	Quantity	Reasons for selection
1	Mild Steel sheet	880mm×440mm×1.5mm	1	Low cost and easily available. Easily machinable Good welding property
2	Stainless steel sheet	480mm×280mm×0.5mm	1	Easily formable to any shape
3	Glass fibre sheet	760mm×760mm×5mm	1	Good transparency property
4	Allen Bolts with washer and nut	6 mm 4mm	30 4	Easily produce Semi-permanent joint
5	Hinges	Mild steel having three holes	2	For easy closing and opening
6	Chloroform	50 ml	1	For easy joint of glass fibre sheet

3.2.1 Enclosure

Generally the abrasive particles are very fine grit size which is remain suspended in the air for very long time. Inhalation of abrasive particles creates seriously respiratory problem on

the lungs and makes disease called silicosis. So the enclosure was made air tight to prevent the mixing of abrasive particle with air.

1 mm thickness of mild steel was taken and was converted into a rectangular box with one sided open by using different operations. For accommodating the transparent glass fiber sheets number of holes were made on the box. Alien bolt was used for tightening purpose. For covering the upper face of the box transparent polythene sheet was used and giving the appropriate allowances .10 mm each side of the edge of polythene is round folded and created a passage. A spring was inserted into the passage for tightening. Then the spring was fixed on the outer side of the box.

3.2.2 Work holding devices

It was designed for holding the work piece. The L-shaped angle plate was designed and bolted it into enclosure. And two flat plates were designed and the work piece was inserted in between the L-plate and flat plate. Then the two plates were tightened by the alien bolt. The holding device was designed such that it can handle the work piece of maximum size i.e. 380×180 mm.

3.2.3 Opening and closing system

Hinge joint was used for opening and closing of the working chamber. The glass fiber was hinge jointed with the enclosure. Hinge was used in mild steel material because of its easy availability and light weight in nature. Two Magnetic clamps were used for tightening the enclosure. Magnetic clamp are combination of two parts, first one is magnet which was fixed in the enclosure and the steel piece was in the movable glass fiber. During the closing, they are in contact and the magnet hold it tightly. The rubber strip was used in the movable glass periphery for providing leak proof closing.

3.2.4 Drainage system

This system is used for safe disposal of abrasive particle. The stainless steel (480mm×280mm×0.5mm) was used for drainage system because it is easily formable and having non corrosive property. The drainage system was made by two way passage system i.e. given slope in both x and y direction. The system was bent in such a way that the total dust particle was collected in one of the corner and a 15mm diameter hole was provided at the corner. For easy removal of abrasive particle a 15.5mm dia steel pipe was welded at this corner.

3.3. Air compressor

Air compressor is shown in the figure 3.3, which compresses air from low pressure to high pressure by taking input energy from electric motor. In AJM, high pressure (2 - 6 bars) air jet is required so that the abrasive particles can strike the work piece at high velocity. In this experiment reciprocating air compressor (maximum pressure= 21 kgf/ cm² or 300 lb/in²) was used for compressing the air. The outlet pressure of compressor is controlled by valve mechanism which is manually control. For running the compressor a new three phase control panel was procured from outside (Schneider electric pvt.ltd).



Fig. 3. 3 Full view of air compressor

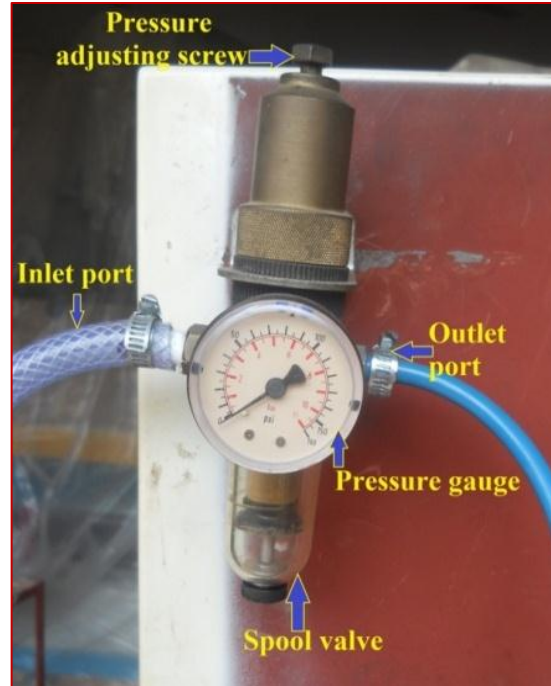


Fig. 3. 4 Full view of FRL unit

3.4. FRL unit

FRL unit (fig. 3.4) stands for filter regulator and lubricator. It is necessary for filtering the air and regulating the air pressure and lubrication of component. The dust particle and moisture particle are suspended in the air. It is necessary for removing the particle otherwise pipeline may result in coagulation and jam the nozzle opening. The pressure is controlled by the pressure regulator, which consists of a loading element, a measuring element and a restricting element. It is a single stage pressure regulator. By rotating the top screw of FRL unit, pressure is controlled within the safe limit. For fixing the upper limit of pressure top screw is necessary.

3.5. Mixing chamber

The mixing chamber (fig. 3.5) contains three parts that is mixing cylinder, cam and motor. It is used for mixing of abrasive powder and compressed air. The torque of motor transformed to cam trough shaft. The cam is touches the bottom of the mixing cylinder. The cam mechanism is used for vibrating the mixing cylinder. The mixing cylinder is hinged to an extension made out of the base. The mixing cylinder was made up of mild steel. the cylinder has three port first one is used for inserting the abrasive particle and it is closed by bolt, second one is used for inlet of compressed air inside the cylinder , third one is used for outlet of mixing of abrasive and air particle. The modeled view of mixing chamber is shown in the fig. 3.6.



Fig.3. 5 Full view of mixing chamber

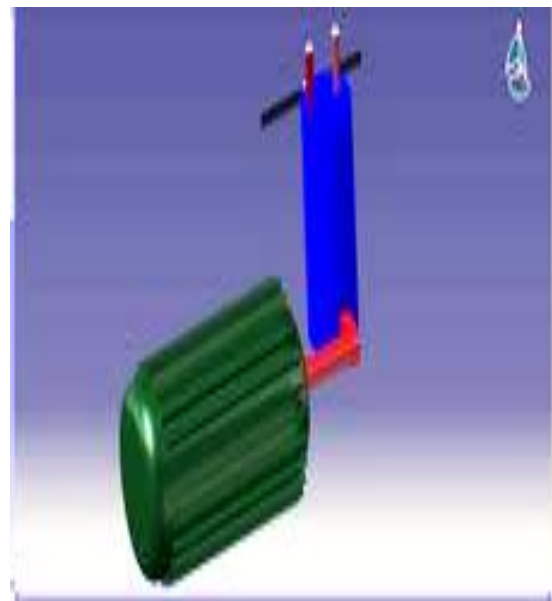


Fig.3. 6 Modeled view of mixing cylinder

3.6. Nozzle and its holding arrangement

For holding the nozzle a holding arrangement was modeled (figure 3.7) and made in the production laboratory .In the fabrication stainless steel alloy nozzle was used, bought from local market. Nozzle holding arrangement (figure 3.8) was designed and fabricated in the institute production laboratory. The nozzle holder was made up of stainless steel sheet, whose thickness is

0.5 mm , having 10mm diameter hole in the center to accommodate nozzle and two 4mm hole in the two side for tightening the arrangement by alien bolt with the C-frame of machine.

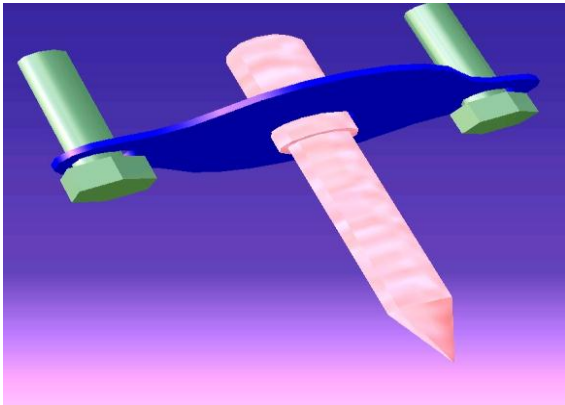


Fig.3. 7 Modeled view of nozzle and its holder

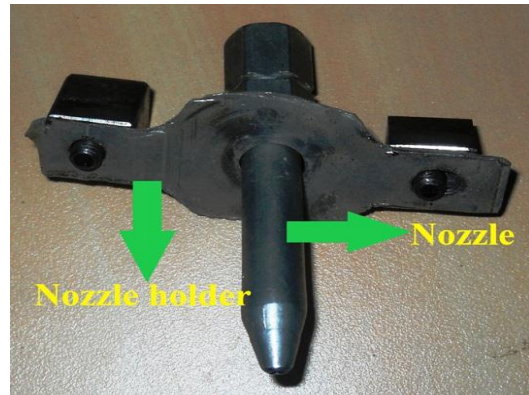


Fig.3. 8 Full view of nozzle and its holder

3.7. Piping circuit

Total piping circuit system was used for smooth flow of compressed air and mixture of compressed air and abrasive powder. Nylon Braided hose pipe (fig. 3.9) having 12mm diameter are used, which is bought from market.



Fig 3. 9 Nylon braided hose pipe

The piping systems are required for carrying the compressed air from the compressor to the mixing chamber and from the mixing chamber to the nozzle orifice via the FRL unit. It is used for its long life, durable, easy available and also having very small head loss when it is bend.

3.8. Machine automation

For involving less human effort and increasing the accuracy of product automation is necessary. By using controller, driver circuit and stepper motor the AJM was automated. The controller generates the electronic pulses and fed to the driver board. The driver board converts electronic pulse into motion control for motor.

3.9. Controller

For movement of X, Y, Z axis controller was needed, which was bought from market. USB6560T4 (fig.3.10) is 4-axies controller device invented by BENTU workgroup, this product is provided to widely diyer in a low price.

Controller have following feature

- USB Interface
- 4-axies on board
- 8 limit switches is allowed to connect to the board for every direction



Fig 3. 10 Full view of controllor

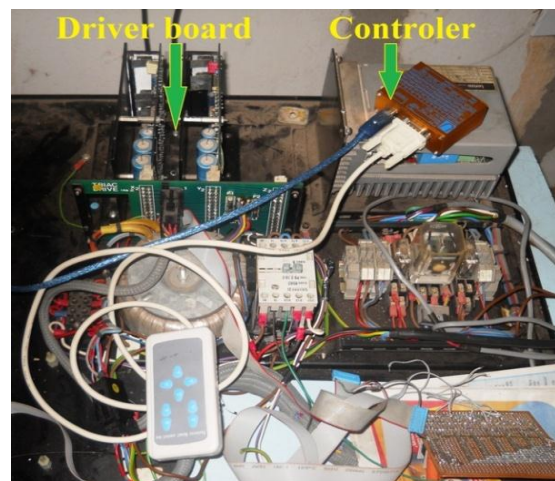


Fig 3. 11 Circuit connection

The controller has two port i.e. USB port and manual control port. USB port is used for controlling the 3-axis through computer. There is a software named as CNC USB

CONTROLLER need to installation. By feeding various programs through the software the axis of machine can move. Also using the manual control port and manual board the axis of machine can move. Back side of controller also having two ports i.e. limit port and step driver port. Limit port is used for limiting the maximum 3-axis movement. And driver port is used for connecting the driver board for driving the stepper motor. Total circuit connection (fig.3.11) was made for rotation of motor.

By using the controller, machine can move in the 3-axis direction and using different types of programing complicated shape was also machined.

3.10. Stepper motor

In this fabrication three stepper motor was used for 3- axis movement which was taken from the old CNC machine. They are mounted on the column and bed .by using led screw arrangement rotary motion of stepper motor is transferred into linear motion. The driver board of the old CNC machine was used, by adding some extra electronic arrangement. The motor specification was given the Table 3.2.

Table 3.2 Motor specification

S.N.	parameter	values
1	voltage	2.9 V
2	Current	3.1 Amps
3	steps	200 Steps/Rev

3.11. Machine Frame and X-Y-Z Travel

The frame of the machine is taken from the CNC milling machine. For holding the nozzle assembly-column is used. The whole machine is mounted on the X-Y table. It is the most important part of the AJM over which the enclosure has to be kept and work piece is machined. The travel of X-Y table is 290 x 170 mm. The X-Y table consists of two parts, (i) Upper table, (ii) Lower table. For x- movement upper table is used and has a travel of 290 mm. and for the y-motion the lower table is used and has a travel of 170 mm

3.12. Assembly

After completing all the component of AJM, assembly was done by taking different tool as per requirement. First modeled assembly (fig.3.13) then full assembly (fig. 3.14) done in the production laboratory.

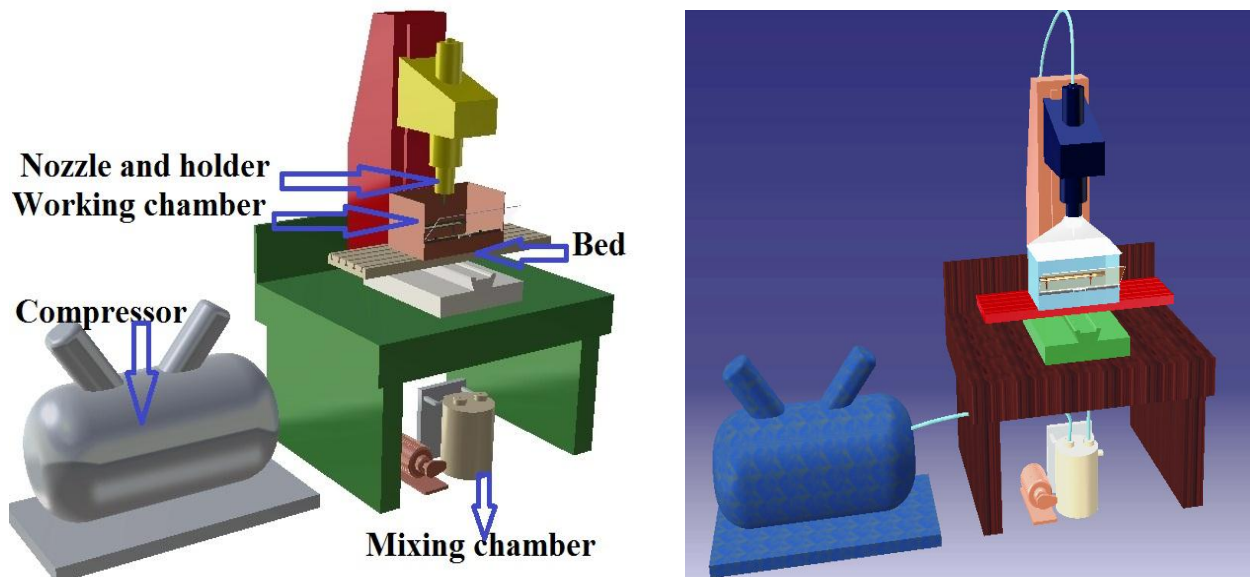


Fig. 3.12 Modeled view of AJM



Fig. 3.13 Front view of AJM



Fig. 3.14 Side view of AJM

3.13. Conclusion

First component was made, and then fabrication was done in our production laboratory. The machine was fully automation by using controller. During the fabrication, different conventional machine tool was used. Care was taken easy and chief available of material in the market and also taking care of available space. Considering their efficiency sometimes procured quality product,.

4.1. Introduction

In this experiment the whole work can be done by Abrasive Jet Machine, which was fabricated in the production laboratory. Atmospheric air used as a medium of carrier gas, aluminum oxide was used as an abrasive powder, Stainless steel alloy nozzle. Glass was taken as a work piece.

4.2. Selection of the work piece and abrasive powder

AJM is capable of machining of hard and brittle material component such as glass, ceramics etc. the properties of glass as shown in table 4.1 and the properties of abrasive powder as shown in the table 4.2.

Table 4. 1 Properties of glass

Chemical composition	SiO ₂ (74%), Na ₂ O (13%), CaO (10.5%), Al ₂ O ₃ (1.3%), K ₂ O (0.3%), SO ₃ (0.2 %), MgO (0.2%) TiO ₂ (0.01%) Fe ₂ O ₃ (0.04%)
Glass transition temperature	573 °c
Density	2400 kg/m ³
Refractive index	1.518

Table 4. 2 Properties of abrasive powder

Composition	Al ₂ O ₃
Appearance	White solid
Odor	odorless
Size	50μ
Density	3.95-4.1gm/cm ³
Solubility	In soluble in water

4.3. Material removal rate

The MRR is defined as the volume of material removed from work piece per unit time. Mechanism of material removal rate of AJM process is most widely established principle is the conversion of mechanical energy into thermal energy. During the process of machining the high velocity jet of abrasive air mixture is bombarded into the glass work piece .The each particle of abrasive powder removes material from work piece.

The MRR is defined as the ratio of the difference of weight of the work piece before and after machining to the product of machining time and density of the material.

$$MRR = \frac{W_b - W_a}{t \times \rho} \dots (4.1)$$

Whereas W_b = Weight of work piece before machining.

W_a = Weight of work piece after machining

Machining time = 1min

Density of glass work piece = 2400 kg/m^3

4.4. Overcut

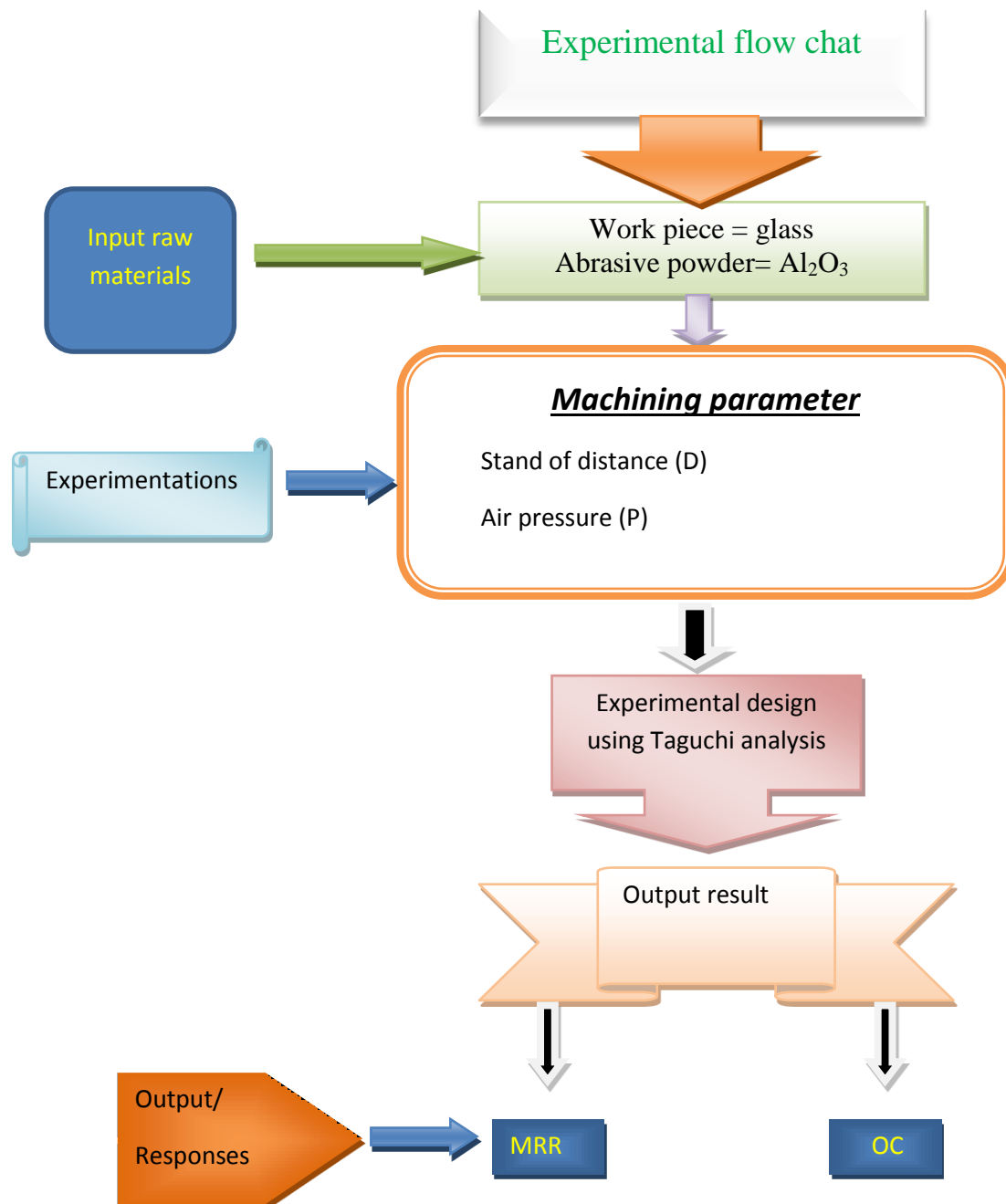
It is the distance by which the machined hole in the work piece exceeds the nozzle bore diameter size. During the process of machining AJM, cavity produced are always larger than the nozzle hole diameter this difference is called Overcut (OC). It becomes important for space application, when close tolerance components are required to be produced.

OC is measured as half the difference of diameter of the hole produced in the work piece to the tool.

$$OC = \frac{D_w - D_t}{2} \dots (4.2)$$

Whereas D_w = diameter of hole produced in the work piece, D_t = Diameter of tool

4.5. Flow Chart of Experiment



4.6. Design of experiments (DOE)

Minitab is software, used for both statistics and dynamic response experiment. The goal of robust experimentation is for finding an optimal combination of control factor settings, Minitab is used. Minitab is relatively easy to use by knowing a few fundamentals. Minitab consists of various method such as factorial, response surface method, mixture, Taguchi method. There are three types of factor which causes the variation in process response [22]. That are controllable factor (can be modified during experimentation), Signal factors (influence the average values of the response but not its variability). Noise factors (influence on the response but which cannot be controlled).

DOE is an experimental strategy, in which the effects of multiple factors are studied by running tests at various levels of the factors. How many experiments should we run, what levels should we take and how to combine them, are subjects of discussions in DOE.

4.7. Taguchi design

Taguchi design is a statistical method, was discovered by Dr. Genichi Taguchi of Japan. It is a robust parameter design, used for designing experiments to calculate how different parameters affect the mean and variance of a process performance characteristic [23]. It is mainly focusing on minimizing variation and sensitivity to noise. It provides an efficient method for designing products and process that operates smoothly, consistently and optimally over a variety of conditions. These methods consist of two, three, four, five, and mixed-level fractional factorial designs. To determine which factors most affect product quality, it allows only the collection of the necessary data thus saving time and resources. Taguchi gives orthogonal array design which reduces the experiment run.

The experimental data are analyzed in the Taguchi method and finding the best response under optimum condition. It is used for estimating the individual factor contribution and also their interaction in the process response. It generates and analysis the main effect plot and interaction plot for signal to noise ratio, means, and standard deviations. It also produces residual plot on histogram, normal plot, and residual versus fits, residual versus order.

By applying the Taguchi Parameter Design techniques, improve the performances of product and process designs in the following ways:

- Improve consistency of performance and save cost
- Build insensitivity (Robustness) towards the uncontrollable factors

In this experiment, a two factor and three levels setup (Table 4.3) is chosen with a total of nine numbers of experiments to be conducted and hence L_9 Orthogonal Array (OA) was chosen.

Table 4. 3 Machining parameters and their level

Factor	Symbol	Unit	Level		
			Level 1	Level 2	Level 3
Stand of distance	(SOD)	mm	0.6	0.8	1.0
Pressure	(P)	bar	2	4	6

4.8. Conduct of experiment

Experimental set up is shown in the fig. 4.1. In this experiment nozzle diameter (2 mm), abrasive particle size (50 μm) is kept constant. The machining parameter Stand of Distance (SOD) and Pressure (P) are varying. For calculating initial and final weight electronic balance weight machine (SHINKO DENSHI Co. LTD, JAPAN, Model: DJ 300S.), which was shown in the fig. 4.2 was used. it has 300 gm. weight capacity and 0.001gm accuracy. The hole dia. of drilled glass piece (fig. 4.4), nozzle dia before experiment (fig 4.5) and nozzle dia. after experiment (fig.4.6) was measurement by tool maker microscope and optical microscope (fig 4.3). In this experiment dia of drilled hole was calculated by taking of the mean dia of both the data two microscope.

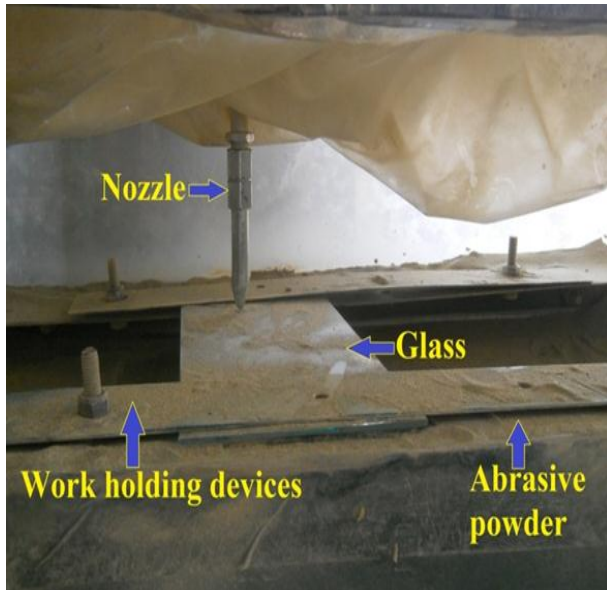


Fig. 4. 1 Experimental set up



Fig. 4. 2 Electronic balance or weight machine



Fig. 4. 3 Optical microscope



Fig. 4. 4 Tool maker microscope

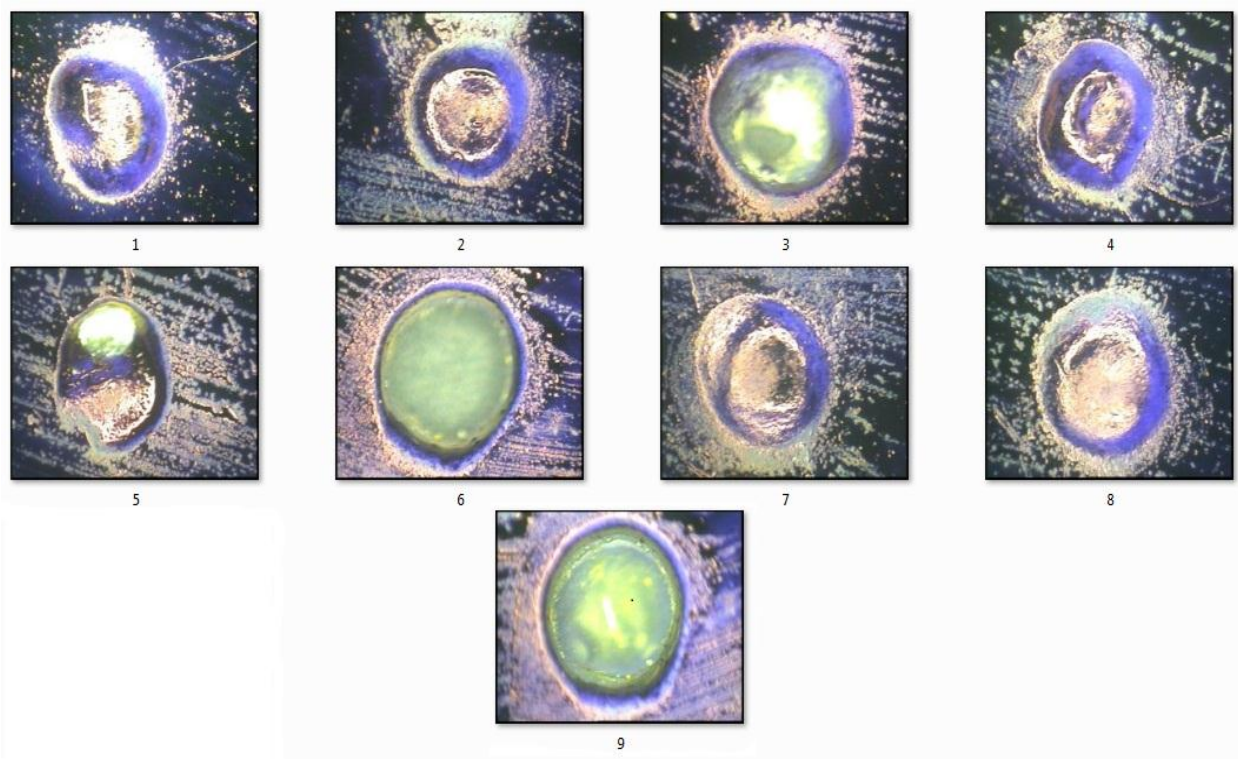


Fig. 4. 5 Drilled cavity on work piece (run numbers are indicated)

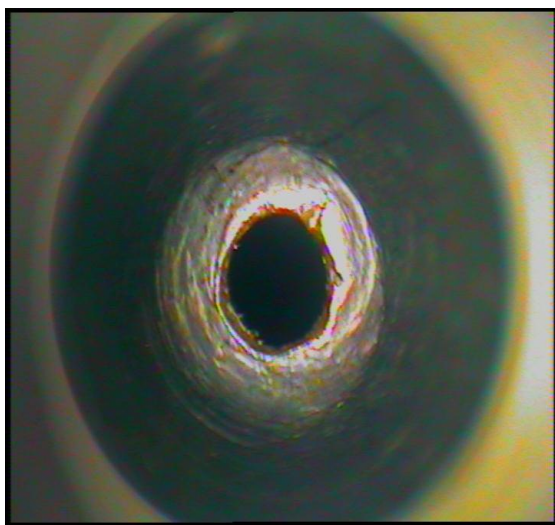


Fig. 4. 6 View of nozzle dia before experiment

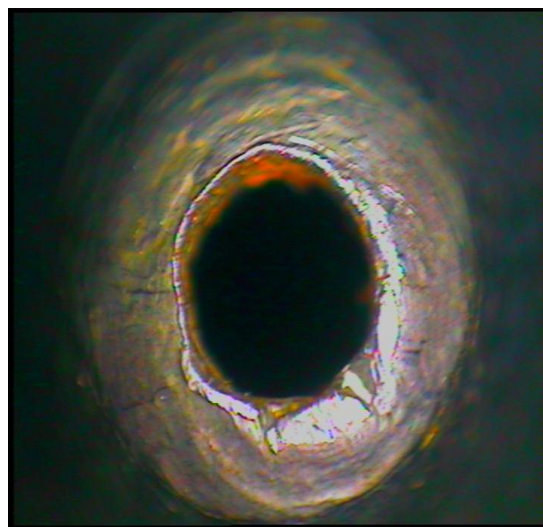


Fig. 4. 7 View of nozzle dia. after experiment

4.9. Design of observation table

The design of Observation table (Table 4.4) was generated by taking the weight of the work piece (initial weight and final weight) and cavity dia of work piece.

Table 4. 4 Design of observation table

Run no	SOD (mm)	P (bar)	Weight of work piece (gm)		Cavity dia (mm)
			Initial weight	Final weight	
1	0.6	2	65.679	65.675	2.265
2	0.6	4	65.674	65.665	2.365
3	0.6	6	65.665	65.648	2.875
4	0.8	2	65.729	65.723	2.290
5	0.8	4	65.723	65.709	2.613
6	0.8	6	65.709	65.684	3.015
7	1.0	2	65.764	65.759	2.320
8	1.0	4	65.759	65.748	2.413
9	1.0	6	65.748	65.729	2.915

4.10. Conclusion

According to Taguchi method, experiments were conducted by using the machining set up. The control parameters like SOD, Pressure were varied to conduct nine different experiments and the weights of the work piece were taken for calculation of MRR and dimensional measurements of the cavity of the work piece were taken for calculation of over cuts (OC).

5.1. Introduction

In this chapter, MRR and OC are calculated by numerical method. And finding the result with process parameter Pressure (P) and SOD is most important with help of Taguchi method.

The machinability of a material in AJM depends on many factors as mixing ratio, nozzle diameter, stand of distance, abrasive particle size, pressure etc. in this analysis pressure and SOD are taken as input parametre.

5.2. Influences of MRR

The observed values of MRR are shown in Table 5.1. During the process of AJM, the influence of machining parameter like SOD and pressure has significant effect on MRR as shown in main effect plot for MRR in fig 5.1. The pressure (p) is directly proportional to MRR in the range of 2 to 6 bar.

Table 5. 1 Observed value of MRR

Run no	SOD (mm)	P (bar)	MRR (mm ³ /min)
1	0.6	2	1.667
2	0.6	4	3.750
3	0.6	6	7.083
4	0.8	2	2.500
5	0.8	4	5.833
6	0.8	6	10.417
7	1.0	2	2.083
8	1.0	4	4.583
9	1.0	6	7.917

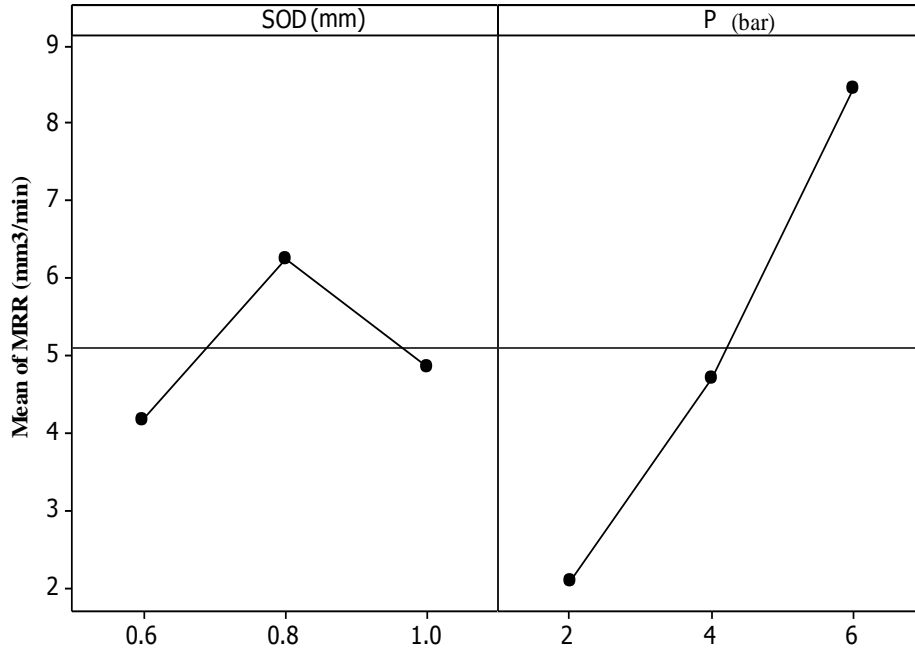


Fig 5. 1 Main effect plot for mean of MRR

This is expected because an increase pressure produces strong kinetic energy which produces the higher temperature, causing more material to erode from the work piece. The other factor SOD does not influence much as compared to pressure. It is clearly indicated from the above fig.5.1 at SOD 0.8mm the MRR was maximum. It decreases with increase in SOD and also decreases with decrease in SOD. It suggests that the effect of one factor is dependent upon another factor.

Sum of square (seq. SS) is necessary to find out the total amount of variation that can be observed by each factor [23].

Degree of freedom (DF) defines the number of independent factor of information involving the response data needed to calculate the sum of squares. Degree of freedom of each component is (n-1) where n is the number of observation observed in this experiment

In an ANOVA the term mean square refer to an estimate of population variance based on the variability among a given set of measures. The calculation for mean square for model term is

$$MS_{Term} = \frac{ADJ\ SST\ term}{DF\ term} \dots\dots (5.1)$$

F-value defines the distance measurement between individual distributions. is inversely proportional to the P-value that means F- value increases the P-value decreases. F-value is used for determine the whether main effect or interaction plot significant or not. Significant.

$$F-Value = \frac{MS\ term}{MS\ error} \dots\dots (5.2)$$

P- value defines the probability of obtaining a test statistic which is significant or not. p value of 0.05 are commonly used.

The analysis of variances for means is shown in Table 5.2, which is clearly indicates that SOD of the nozzle is not important for influencing MRR and pressure (p) is the most influencing factors for MRR. The delta values are pressure (p) and SOD 6.389 and 2.083 respectively, depicted in Table 5.3. The case of MRR, it is “Larger is better”, so from this table it is clearly definite that pressure is the most important factor then SOD, From the % of contribution it is shown in the table 5.2 that the p has 87.87 % contribution, SOD have 9.59 % contribution and error comes 2.57 % .

Table 5. 2 Analysis of variance for MRR

Source	DF	Seq SS	Adj MS	F	P	% Contribution
SOD	2	6.752	3.3758	7.44	0.045	9.59
P	2	61.847	30.9234	68.19	0.001	87.84
Residual Error	4	1.814	0.4535			2.57
Total	8	70.413				

Table 5. 3 Response table for MRR

Level	SOD	P
1	4.167	2.083
2	6.250	4.722
3	4.861	8.472
Delta	2.083	6.389
Rank	2	1

From the estimated model coefficient for means table 5.4, The R^2 parameter indicates that the amount of variation observed on MRR is explained by the input factors. $R^2 = 97.4\%$ indicate that the model is able to predict the high accuracy response. R^2 Adjusted is also called a R^2 modified that has been adjusted for the number of terms in the model. If unwanted terms are included in the model, R^2 (=97.4 %) can be artificially high, but R^2 adjusted (=94.8 %) may be smaller. In the modeling, the standard deviation of errors $S = 0.6734$.

Table 5. 4 Estimated Model Coefficients for MRR

Term	Coef	SE Coef	T	P
Constant	5.0926	0.2245	22.686	0.000
SOD 0.6	-0.9259	0.3175	-2.917	0.043
SOD 0.8	1.1574	0.3175	3.646	0.022
P 2	-3.0092	0.3175	-9.479	0.001
P 4	-0.3706	0.3175	-1.167	0.308
S = 0.6734 R-Sq = 97.4% R-Sq(adj) = 94.8%				

Comparing the p-value with the α -value (= 0.05), it is observed that if the p-value is less than or equal to α , then the effect is significant otherwise it is not significant. From the above figure it is indicates that SOD and P both are significant. The residual plot for mean of MRR is

shown in Fig. 5.2. This diagram is very useful to calculate whether the model meets the assumptions of the analysis or not.

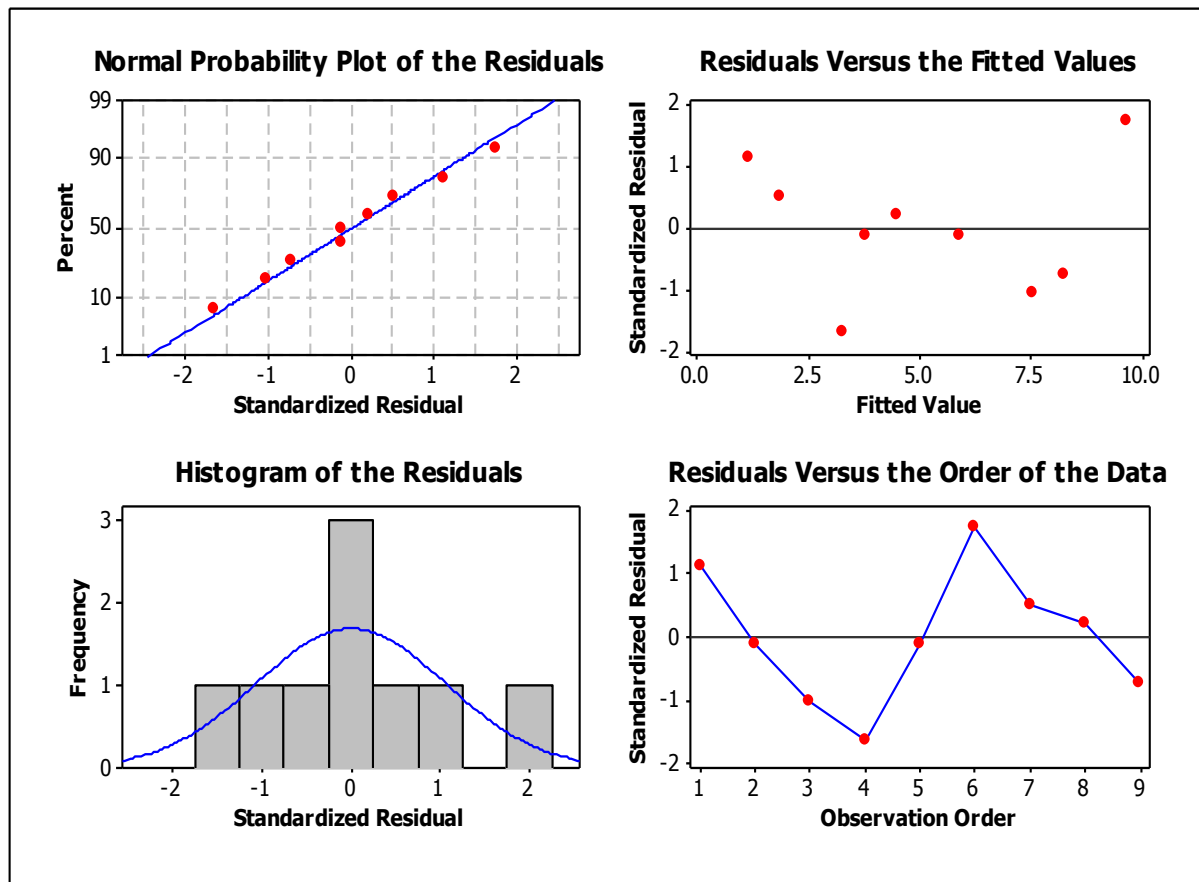


Fig 5. 2 The residual plot for mean of MRR

The residual plots of the graph given below:

- Normal probability plot of the residual signifies that the data are normally distributed and the variables are influencing the response [24]. Standardized residues data are existing in between -2 and 2.
- Residuals versus fitted curve signify that the variance is constant, a nonlinear relationship exists in the data and no outliers exist in the data.
- Histogram of the residual indicates that the data are not outliers and not skewed exist.
- Residuals versus order of the data signify that there are systematic effects in the data due to time or data collection order.

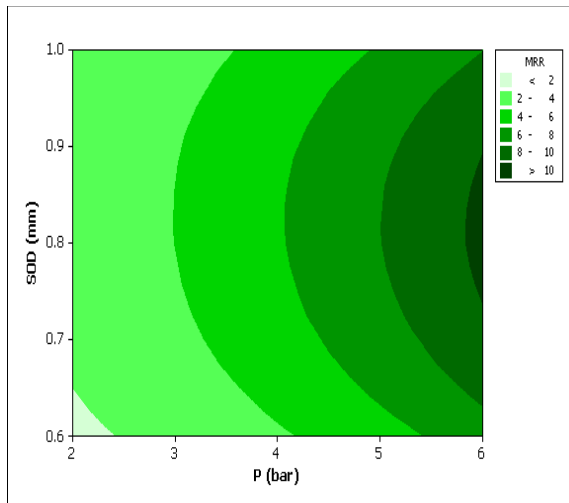


Fig. 5. 3 Contour plot of MRR

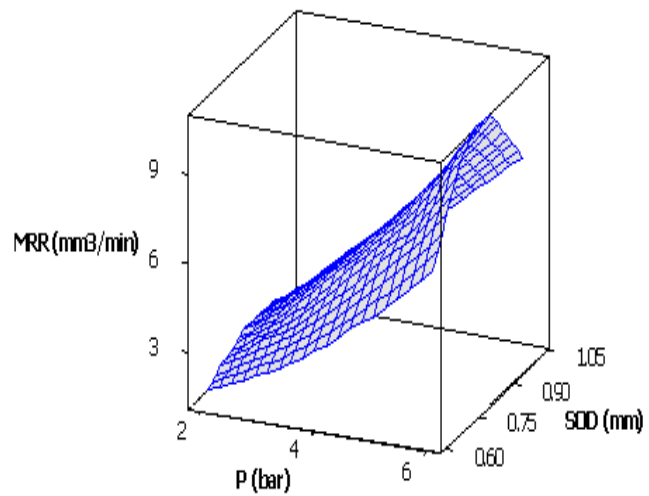


Fig 5. 4 Surface plot of MRR

In fig. no.5.3 Contour plot of MRR (SOD versus P) shows that the MRR is maximum when pressure is maximum and MRR is maximum when SOD is in the range 0.7 to 0.9mm.

From the above surface plot of fig 5.4, shows that see that MRR is increases rapidly with pressure and MRR is maximum in the region of SOD (0.75-0.9 mm)

5.3. Influences of OC

The observed values of OC are shown in Table 5.5. During the process of AJM, the influence of machining parameter like SOD and pressure has significant effect on OC, as shown in main effect plot for OC that is Fig. 5.5. The pressure (p) is directly proportional to OC in the range of 2 to 6 bar.

Table 5.5 Observed value of OC

S.N.	SOD(mm)	P(bar)	OC(mm)
1	0.6	2	0.1325
2	0.6	4	0.1825
3	0.6	6	0.4375
4	0.8	2	0.1450
5	0.8	4	0.3065
6	0.8	6	0.5075
7	1.0	2	0.1600
8	1.0	4	0.2065
9	1.0	6	0.4575

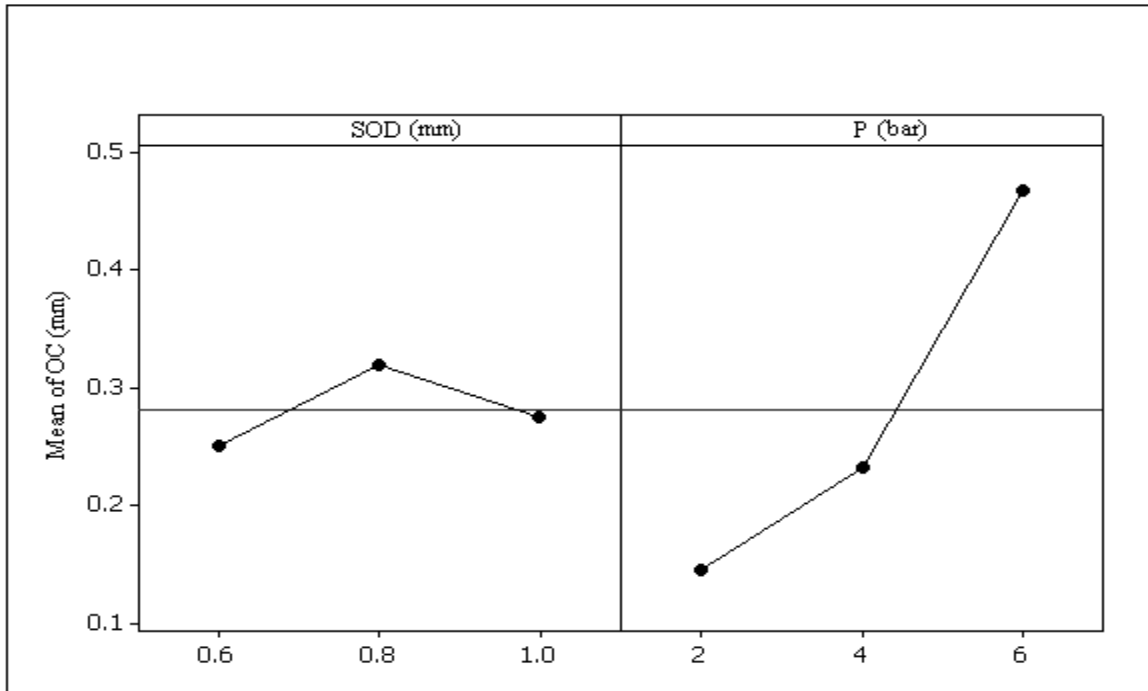


Fig. 5.5 Main effect plot of mean for OC

This is expected because an increase pressure produces strong kinetic energy which produces the higher temperature, causing more material to erode from the work piece and also make OC higher.

The other factor SOD also influences on the OC. It is clearly indicated from the above figure at SOD 0.8mm the OC was maximum. It decreases with increase in SOD and also decreases with decrease in SOD.

The analysis of variances for the factors is shown in Table 5.6 .which is clearly indicates that both SOD of the nozzle and pressure also important for influencing OC The delta values are pressure (p) and SOD 0.3217 and 0.0688 respectively, depicted in Table 5.7. The case of OC, it is “Smaller is better”, so from this table it is clearly define that pressure is the most important factor then SOD, this is also conform that response table of means that’s shown in same table. From the % contribution of p has 93.47 %. SOD have 4.12 % contribution and error comes 2.41 % .

Table. 5. 6 Analysis of Variance for OC

Source	DF	Seq SS	Adj MS	F	P	% Contribution
SOD	2	0.007331	0.003666	3.41	0.137*	4.12 %
P	2	0.166404	0.083202	77.42	0.001	93.47 %
Residual Error	4	0.004299	0.001075			2.41 %
Total	8	0.178034				
* Indicates the insignificant factor						

Table 5. 7 Response Table for OC

Level	SOD	P
1	0.2508	0.1458
2	0.3197	0.2318
3	0.2747	0.4675
Delta	0.0688	0.3217
Rank	2	1

From the estimated model coefficient for table 5.8. The R^2 parameter indicates that the amount of variation observed on MRR is explained by the input factors. $R^2 = 97.6\%$ indicate

that the model is able to predict the high accuracy response. R^2 Adjusted is also known as a R^2 modified that has been adjusted for the number of terms in the model. If unwanted terms are included in the model, R^2 (97.6 %) can be artificially high, but R^2 adjusted (=95.2 %.) may be smaller. In the modeling, the standard deviation of errors $S = 0.03278$.

Table 5. 8 Estimated Model Coefficients for OC

Term	Coef	SE Coef	T	P
Constant	0.28172	0.01093	25.781	0.000
SOD 0.6	-0.03089	0.01545	-1.999	0.116
SOD 0.8	0.03794	0.01545	2.455	0.070
P 2	-0.13589	0.01545	-8.793	0.001
P 4	-0.04989	0.01545	-3.228	0.032
S = 0.03278 R-Sq = 97.6% R-Sq(adj) = 95.2%				

Comparing the p-value with the α -value (= 0.05), it is observed that if the p-value is less than or equal to α , then the effect is significant otherwise it is not significant. From the above figure it is indicates that SOD is insignificant and P are significant.

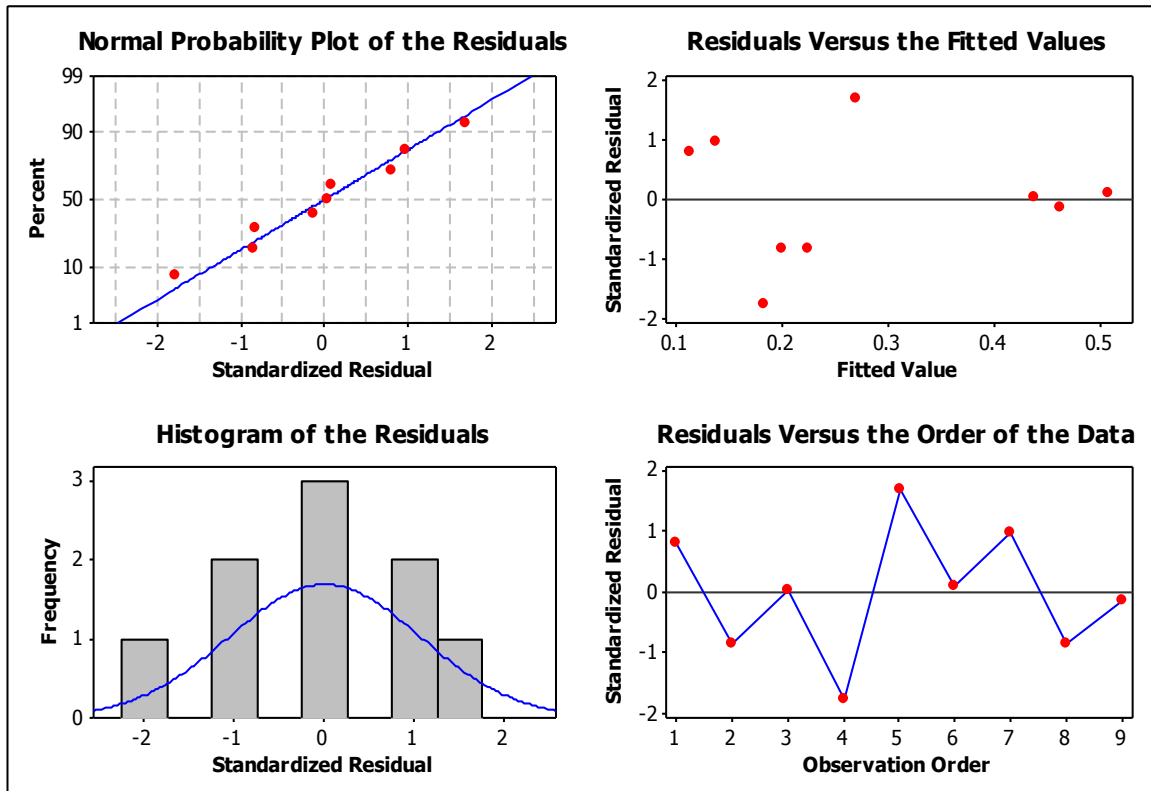


Fig. 5. 6 Residual plot for OC

The residual plot for OC is shown in fig 5.6. This diagram is very useful to calculate whether the model meets the assumptions of the analysis or not.

The residual plots in the graph given below:

- Normal probability plot of the residual signifies that the data are normally distributed and the variables are influencing the response. Standardized residues data are existing in between -2 and 2.
- Residuals versus fitted curve signify that the variance is constant, a nonlinear relationship exists in the data and no outliers exist in the data.
- Histogram of the residual indicates that the data are not outliers and not skewed exist.
- Residual versus order of the data signifies that there are systematic effects in the data due to time or data collection order.

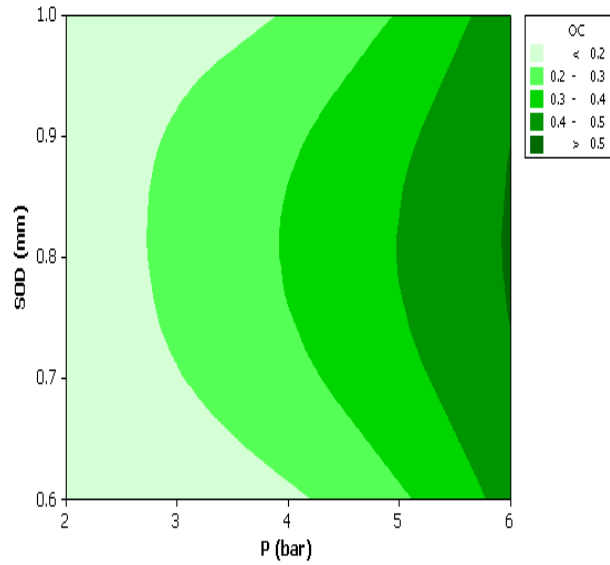


Fig. 5. 7 Contour plot for OC

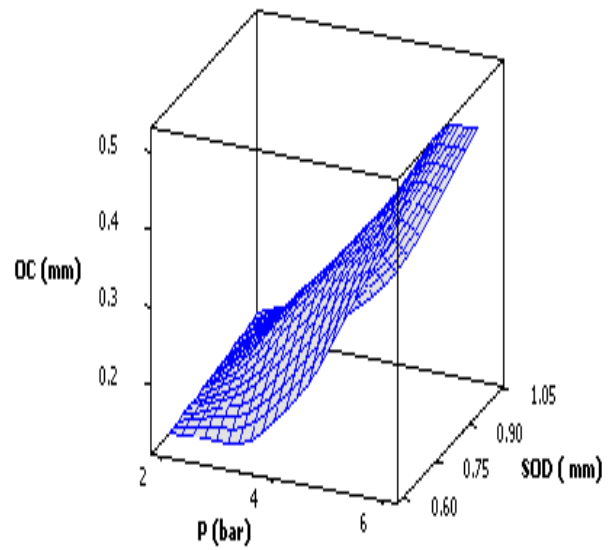


Fig 5. 8 Surface plot for OC

From the above contour plot of OC fig 5.7. (SOD verses P) shows that the OC is minimum when pressure is in between 2-3 bar and OC is maximum when SOD is in the range 0.7 to 0.9 mm. From the above surface plot fig 5.8.shows that see that OC is increases rapidly with pressure and OC maximum in the region of SOD (0.75-0.9 mm)

5.4. Conclusion

The observed value of MRR and OC was analyzed by Taguchi design. From analysis it was concluded that the pressure and SOD both are significant for MRR and only pressure is significant for OC.

In this research work, AJM fabrication was done and later drilling experiment was carried on the glass work piece. During the fabrication and experiment following conclusion was derived.

6.1. Conclusion based on fabrication work

1. A completed CAD model of AJM was prepared considering the optimum use of available material and space.
2. Working chamber, nozzle holder arrangement, work holding device were made in our production laboratory
3. The AJM is can be used for drilling and milling of glass plates or other brittle materials.
4. By feeding different type of programing on controller, various complicated shapes are machined.
5. Experimental work was done by considering SOD and Pressure are machining parameter to study MRR and OC.
6. For MRR both SOD and pressure are significant factor and for OC only pressure is significant.
7. MRR is increases with increase in pressure. For increase in SOD firstly MRR increases then it is remain constant after that it is decreases.

6.2. Scope for future work

1. A precision AJM will be designed by using gear mechanism, Solenoid valve, crankshaft, springs and flexure etc.
2. More number of experiment will be done by using different type of ceramic nozzle such as tungsten carbide, boron carbide etc.
3. Machining operation will be conducted on the brittle and nonconductive material
4. Changing different type of abrasive powder with its grain size experimental work will be done.

References

1. Juan-Hung Kea, Feng-Che Tsaia, Jung-Chou Hungb, Biing-Hwa Yanc, (2012) “Characteristics study of flexible magnetic abrasive in abrasive jet machining,” *Procedia CIRP*, Vol. 1, pp. 679 – 680.
2. H.Z. Li, J. Wang, J.M. Fan, (2009) “Analysis and modelling of particle velocities in micro-abrasive air jet,” *International Journal of Machine Tools & Manufacture*, Vol. 49, pp. 850–858.
3. A.G. Gradeena, J.K. Spelta, M. Papinia, (2012) “Cryogenic abrasive jet machining of polydimethylsiloxane at different temperatures,” *wear*, Vol. 274-275, pp. 335-344.
4. S. Ally , J.K. Spelt , M. Papini, (2012) “Prediction of machined surface evolution in the abrasivejet micro-machining of metal,” *wear*, Vol. 292-293, pp. 89-99.
5. R.K. Tyagi, (2012) “Abrasive jet machining by means of velocity shear instability in plasma.” *journal of manufacturing process*,” Vol. 14, pp. 323-327.
6. Y. Lin, Y. Chen, A. Wang, W. Sei (2012), “Machining performance on hybrid process of abrasive jet machining and electrical discharge machining,” *Transactions of Nonferrous Metals Society of China (English Edition)*, Vol. 22, pp. 775-780.
7. D. Dehnadfar, J. Friedman, M. Papini (2012), “Laser shadowgraphy measurements of abrasive particle spatial, size and velocity distributions through micro-masks used in abrasive jet micro-machining,” *Journal of Materials Processing Technology*, Vol. 212, pp. 137- 149
8. J.M. Fan , H.Z. Li , J. Wang , C.Y. Wang (2011), “A study of the flow characteristics in micro-abrasive jets,” *Experimental Thermal and Fluid Science*, Vol. 35, pp. 1097-1106.
9. H. Getu , J.K. Spelt , M. Papini (2011), “Thermal analysis of cryogenically assisted abrasive jet micromachining of PDMS,” *International Journal of Machine Tools & Manufacture*, Vol. 51, pp. 721-730.
10. T. Burzynski, M. Papini (2011) , “ A level set methodology for predicting the surface evolution of inclined masked micro-channels resulting from abrasive jet micro-machining at oblique incidence,” *International Journal of Machine Tools & Manufacture*, Vol. 51, pp. 628-641.

11. Lei Zhang, Tsunemoto Kuriyagawa, Yuya Yasutomi, Ji Zhao (2005), "Investigation into micro abrasive intermittent jet machining, International Journal of Machine Tools & Manufacture, Vol. 45, pp. 873-879.
12. A. Ghobeitya, M. Papinib, J.K. Spelta (2009), "Abrasive jet micro-machining of planar areas and transitional slopes in glass using target oscillation," Journal of Materials Processing Technology, Vol. 209, pp. 5123-5132.
13. M. Wakuda , Y. Yamauchi , S. Kanzaki (2002), "Effect of workpiece properties on machinability in abrasive jet machining of ceramic materials," Journal of the International Societies for Precision Engineering and Nanotechnology, Vol. 26, pp. 193-198.
14. Dong-Sam Park , Myeong-Woo Cho , Honghee Lee , Won-Seung Cho (2004), "Micro-grooving of glass using micro-abrasive jet machining," Journal of Materials Processing Technology, Vol. 146, pp. 234-240.
15. N. Shafiei, H. Getu, A. Sadeghian, M. Papini (2009), "Computer simulation of developing abrasive jet machined profiles including particle interference," Journal of Materials Processing Technology, Vol. 209, pp. 4366-4378.
16. Massimiliano Barletta, Vincenzo Tagliaferri (2006), "Development of an abrasive jet machining system assisted by two fluidized beds for internal polishing of circular tubes," International Journal of Machine Tools & Manufacture, Vol. 46, pp. 271-283.
17. H.Z. Li, J. Wang, J.M. Fan (2009), "Analysis and modelling of particle velocities in micro-abrasive air jet," International Journal of Machine Tools & Manufacture, Vol. 49, pp. 850-858.
18. Deng Jianxin, Wu Fengfang, Zhao Jinlong (2007), "Wear mechanisms of gradient ceramic nozzles in abrasive air-jet machining," International Journal of Machine Tools & Manufacture, Vol. 47, pp. 2031-2039.
19. R. Haj Mohammad Jafar , J.K. Spelt , M. Papini (2013), "Numerical simulation of surface roughness and erosion rate of abrasive jet micro-machined channels, wear, Vol. 303, pp.302-312.
20. M. Achtsnick , P.F. Geelhoed , A.M. Hoogstrate , B. Karpuschewski (2005), "Modelling and evaluation of the micro abrasive blasting process," wear, Vol. 259, pp. 84-94.

21. Deng Jianxin (2005), "Erosion wear of boron carbide ceramic nozzles by abrasive air-jets," Materials Science and Engineering A, Vol. 408, pp. 227-233.
22. Minitab14 (2003) Minitab user manual Release 14. State College, PA, USA.
23. P. J. Ross (1988), "Taguchi techniques for quality engineering" McGraw-Hill, New York.
24. Shailesh Dewangan (2008), M-Tech thesis, thesis NIT Rourkela.

BIBLIOGRAPHY

1. www.nptel.iitm.ac.in
2. www.wikipedia.org
3. [www.sand-blasting.co/the-history-of-sand blasting](http://www.sand-blasting.co/the-history-of-sand-blasting).
4. ezinearticles.com › Reference and Education
5. http://EzineArticles.com/?expert=Andy_McCarthy